Experimental Study of Shear and Tensile Properties of LIGA Ni-Fe and Ni-Co Alloys at Quasi-static and Intermediate Strain Rates

19

Li-Anne Liew, David T. Read, May L. Martin, Todd R. Christenson, Peter E. Bradley, Nicholas Barbosa, Frank W. DelRio, Jeffrey R. Smyth, and John T. Geaney

Abstract

We report the in-plane shear properties, to fracture, of 200 μm-thick LIGA nanocrystalline Ni-10%Fe and micrograined Ni-10%Co. Planar simple shear specimens were designed, fabricated and pulled to fracture using a miniature commercial tension test stage. Forces were measured with a load cell and displacements were measured via digital image correlation. A procedure was developed to extract the shear strains from the displacements. We show shear stress vs shear strain curves to fracture for each material, at strain rates 0.001/s and 30/s. Tensile tests were also performed on both materials at strain rates 0.001/s and 1/s. Increases in shear strength, tensile strength, and true strain to fracture were observed at the higher strain rate, but rate effects were inconclusive for the Young's modulus, shear modulus, and yield strength due to large measurement uncertainties. Finally, the stress triaxiality and equivalent plastic strain at fracture for the tensile and shear specimens were estimated and used to construct part of the fracture locus for the Ni-10%Fe material. It is anticipated that this data may be used to facilitate failure prediction models for LIGA MEMS.

Keywords

Electrodeposited nickel, LIGA · MEMS, Shear, Fracture locus

19.1 Introduction

The commercialization of Micro Electro Mechanical Systems (MEMS) in a growing number of industries has resulted in an increased emphasis on MEMS structural reliability and accurate failure prediction models. To this end, material data under various loading conditions and with well-understood uncertainties are needed to construct and validate material constitutive models. Many works over the past two decades have reported the mechanical properties of films of Ni and its alloys fabricated through the LIGA process. LIGA [1, 2] is a German acronym for Lithographie, Galvanoformung, Abformung, meaning lithography, electroplating and molding. However, while tensile, fatigue, bending, creep and fracture toughness properties

L.-A. Liew (✉) · D. T. Read · M. L. Martin · P. E. Bradley · N. Barbosa
Applied Chemicals and Materials Division, National Institute of Standards and Technology, Boulder, CO, USA
e-mail: li-anne.liew@nist.gov

F. W. DelRio
Sandia National Laboratories, Albuquerque, NM, USA

T. R. Christenson
HT MicroAnalytical, Albuquerque, NM, USA

J. R. Smyth · J. T. Geaney
U.S. Army Combat Capabilities Development Command Armaments Center, Picatinny Arsenal, NJ, USA

of LIGA alloys have been given attention in the literature, far fewer papers to date report their shear properties to fracture or the fracture locus of LIGA materials. Two examples of shear property measurements include Refs [3, 4] which reported the shear modulus of silicon and LIGA Ni using torsional specimens that were twisted out of plane by bench-top loading apparatuses, and the angular displacement was measured optically, but while the torsional test of the silicon specimens resulted in fracture, the test on the LIGA Ni was not to fracture. In-plane torsional tests have been performed, to fracture, on single crystal silicon pillars with cross sectional areas of about 1 um², through use of in-situ fabricated silicon MEMS actuators for applying the loads [5]. Micro-torsional tests have been used to measure the shear modulus of other MEMS materials, see for example the recent review of micro-mechanical test techniques in Ref [6]. With micro-torsional test techniques, however, shear tests, especially to fracture, are technically challenging and typically not performed for ductile materials, and shear strains are difficult to measure when there is extensive plastic deformation.

We conducted a detailed experimental study of the in-plane shear properties, to fracture, of two LIGA alloys: a high-strength nanocrystalline Ni-10%Fe alloy and a ductile micrograined Ni-10%Co alloy. Unlike the previous work on the LIGA Ni shear modulus and most of the MEMS materials literature, our shear test approach did not involve torsional loading. Instead, we drew from the tradition of macroscale sheet metal studies and used planar specimens (200 μm thick, and with gauge width of 600 μm) that were loaded in tension to produce near-pure shear stresses in the center of the specimen. Since the LIGA fabrication process is planar and results in anisotropy in microstructure and properties due to electrodeposition, LIGA MEMS devices under complex loading are likely to experience in-plane shear stresses, thus planar specimens would more accurately capture the material behavior in these conditions. Other advantages of planar specimens over micro-torsional specimens are that the stress state stays constant to larger deformations, tests to fracture and at various strain rates can be more easily performed, and shear strength and yield strength in shear can be directly measured. We also conducted tensile tests on specimens with gauge sections 2 mm long × 200 μm wide × 200 μm thick, with more details in Refs. [7, 8]. We report here the shear and tensile properties of the two alloys, at two strain rates, and show part of the fracture locus of the nanocrystalline Ni-10%Fe alloy, constructed from the fracture strains of the tensile and shear specimens. This data can potentially be used to construct or validate failure prediction models for LIGA MEMS.

19.2 Experimental Methods

The textbook definition of simple shear for a material of width, W, along the y-axis, is illustrated in Fig. 19.1a for the xy Cartesian coordinate system. When a displacement, $u = \Delta x$, is applied, an angle, α, is formed. The simple shear strain, γ, is given by:

$$\gamma = \tan(\alpha) = \frac{\Delta x}{W} \tag{19.1}$$

Much work has been done over the past several decades in developing and analyzing designs of planar simple shear specimens of various materials and developing test procedures at the macroscale. We based our specimen design on a scaled down version of ASTM B831 [9], which is a standard for shear testing of sheet metals. However, the ASTM design, shown in Figs. 19.1b, c, calls for the gauge section to be thinner than the rest of the specimen. The width of the reduced section ("W" in Fig. 19.1c) can be taken as W in Fig. 19.1a and Eq. 19.1. Our specimens, on the other hand, were designed as a single layer
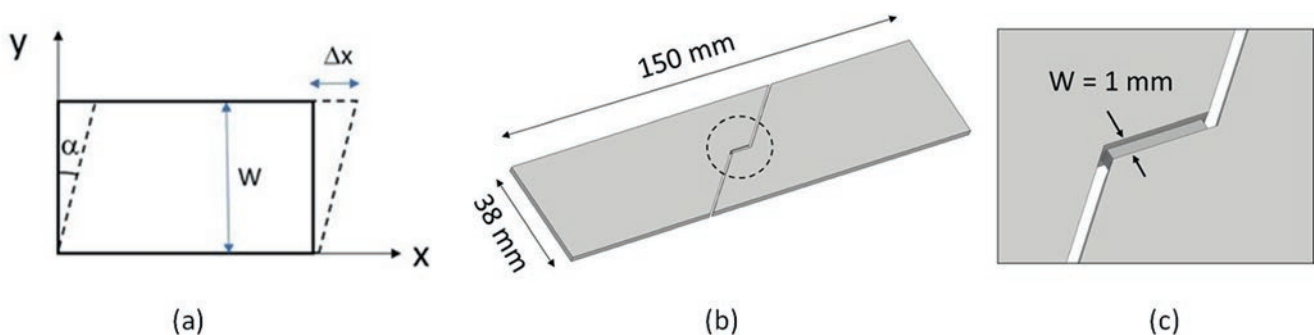

Fig. 19.1 (**a**) Definition of simple shear strain, $\gamma = \tan \alpha = (\Delta x)/W$. (**b**) Solid model of ASTM B831 specimen [9, 10], the total thickness is 2 mm. (**c**) Close up of the reduced gauge section in (**b**), with dimensions 6.35 mm long × 1 mm wide × 1 mm thick

Fig. 19.2 (**a**) Photograph of a shear specimen beside a millimeter ruler. The specimens were 200 μm thick. (**b**) Optical micrograph of the gauge section
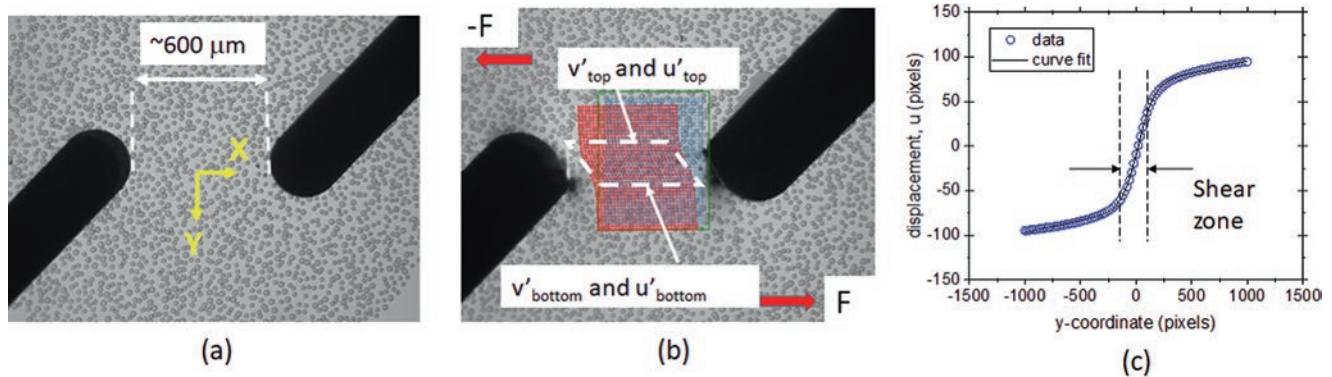

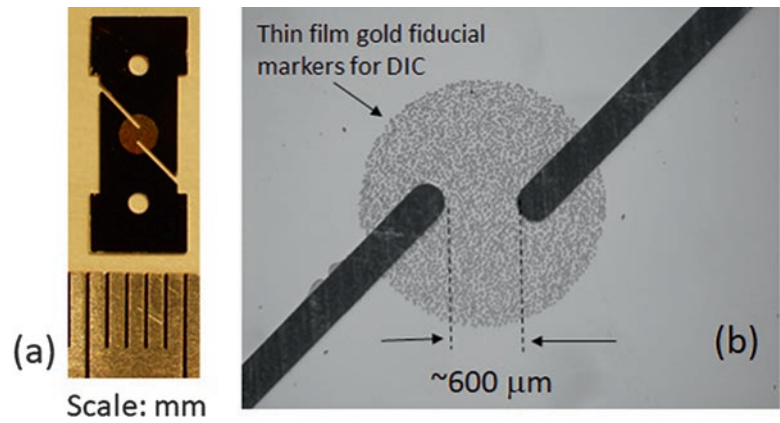**Fig. 19.3** Optical micrographs from a shear test, (**a**) at the start of the test (**b**) during simple shear deformation with the DIC grid overlayed, where *u* is the displacement in *x*, *v* is the displacement in *y*, and *u'* and *v'* are these displacements after a correction for rigid-body rotation has been applied. The trapezoid (dotted lines) was drawn manually to represent the shear zone and is meant to guide the eye only. (**c**) Typical displacement in the *x*-direction (*u*) vs. *y*-position, for one image

of uniform thickness to reduce the LIGA fabrication complexity. This design change made the measurement of the shear strain more challenging, as described later in this section. A typical specimen is shown in Fig. 19.2. As shown in Fig. 19.2b, an array of 25 um-diameter and 1 um-thick Au dots was deposited and patterned on the surface of the gauge section to create a speckle pattern to facilitate the use of digital image correlation (DIC) for strain measurement [7].

The specimens were pulled apart at strain rate 0.001/s in a commercial table-top miniature tension stage mounted under an optical microscope. Force was measured with a 334 N (75-lb) load cell, and optical micrographs of the gauge sections were captured by a CCD camera. For the higher rate tests, a larger commercial bench top load frame with a 5 kN load cell was used, with a high-speed camera for acquiring images. More details of the test apparatus are in [7]. The specimen thicknesses were measured, before testing, with a digital micrometer at the grip sections. The gauge width, designed at 600 μm, was measured from optical micrographs. The engineering shear stress was calculated as the force divided by the gauge section's initial cross-sectional area. Figures 19.3a, b show the gauge section of a specimen before and during a shear test. DIC, using a custom program, was used to measure the displacements across the gauge section. The forces and images were analyzed off line to construct the engineering shear stress vs. shear strain curves.

The ASTM B831 standard [9] defines the calculation of the simple shear strain from measurable quantities (displacements) using Eq. 19.1. However, since our specimens were of uniform thickness, the gauge width *W* in Eq. 19.1 and Fig. 19.1a was neither physically defined nor constrained as in the ASTM design (compare Fig. 19.3a with Fig. 19.1c) but instead would evolve during the course of a test. Determining the shear strain in our specimens was thus considerably more involved than in the ASTM standard. Our approach was to plot the DIC displacements (*u*) in the direction of shear, with respect to the transverse position, *y*, averaged across the DIC grid shown in Fig. 19.3b. From the resulting displacement plot (Fig. 19.3c), the slope of the linear section of the "S" shaped curve is the simple shear strain, γ. As the shear test proceeds, the "S" shaped curve evolves in size and slope. To automate the extraction of γ from all the images, a custom program was written to perform an empirical fit to the displacements using a hyperbolic tangent function:

$$u_{predicted} = y_0 + m(x - x_0) + C tanh[D(x - e)] \tag{19.2}$$

where $u_{predicted}$ is the predicted value of the displacement, x is the independent variable which in this case is the y-coordinate in the DIC images, x_o is the starting y-coordinate at the beginning of the data set, and y_o, m, C, D, and e are constants found by nonlinear regression. The shear strain is then extracted by the program as:

$$\gamma = CD \tag{19.3}$$

In addition to the shear specimens, we also designed, fabricated and tested tensile specimens with gauge section dimensions of 2 mm long × 200 μm wide × 200 μm thick. The tensile specimens were of the same materials as the shear specimens but were fabricated in a separate fabrication run. The same testing apparatus was used as for the shear tests, and the same DIC program was used to measure the engineering strain from the displacements at the ends of the gauge sections. Details of the tensile tests are reported elsewhere [7, 8].

19.3   Results and Discussion

Figure 19.4 shows representative engineering shear stress versus simple shear strain curves, to fracture, for the two LIGA alloys, at strain rates of 0.001/s and 30/s. The Ni-10%Fe shows much higher shear strength while the Ni-10%Co alloy exhibits much higher ductility. The measurement uncertainty in the shear stress is under 2%. The measurement uncertainty in the shear strain for the Ni-Fe is within ~7%. The shear strain values for the Ni-Co alloy (Fig. 19.4b) are within ~4% uncertainty until the maximum shear stress. After the maximum stress is reached, as the ductile Ni-10%Co continues to be pulled apart the gauge section undergoes extensive plastic deformation, such that the deformation profile starts to deviate from the simple shear defined in Fig. 19.1, this deviation reaching a maximum of 35–40% at fracture. Nevertheless, the curves for the Ni-10%Co alloy are plotted for all strain values until fracture, for comparison with the Ni-10%Fe.

Figure 19.5 shows the fracture surfaces of a shear specimen of each material, tested at the lower strain rate. The Ni-Fe alloy (Fig. 19.5a) fails in a brittle manner, while the Ni-Co alloy (Fig. 19.5b) fails in a ductile manner. The fracture surfaces of *tensile* specimens of the same materials show similar characteristics [11]. The fracture mechanisms of the two alloys are discussed in detail in Ref [11].

Table 19.1 summarizes the shear and tensile properties of the two LIGA alloys, at two strain rates: a quasi-static strain rate of 0.001/s, and an intermediate strain rate of 30/s for the shear specimens, and 1/s for the tensile specimens. The tensile properties are discussed in more detail in [7, 8]. All nominal values in Table 19.1 are averaged over 6 shear specimens per material/rate combination, and 3 tensile specimens per material/rate combination. The uncertainties reported are the measurement uncertainties, calculated from error analysis, with the exception of the tensile specimens' true strain to fracture where the uncertainty is the standard deviation. Both materials exhibit an increase in the shear strength, tensile strength, and true strain to fracture, with increasing strain rate. The nominal values of the Young's modulus and shear modulus appear to
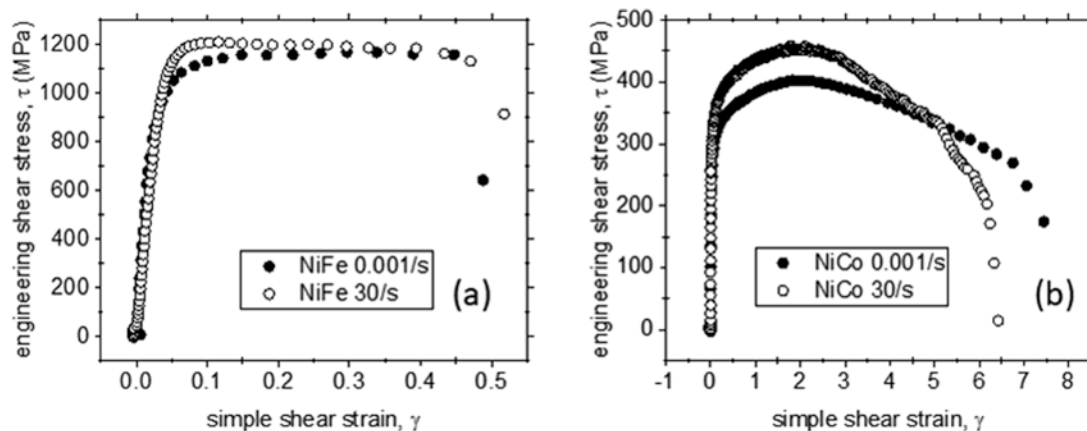

Fig. 19.4 Shear stress vs shear strain curves, to fracture, for (**a**) nanocrystalline Ni-10%Fe, (**b**) micrograined Ni-10%Co. For (**b**), the shear strains beyond the maximum shear stress are not accurate due to up to 40% deviation from simple shear in the specimen during the test. The curves are nonetheless plotted to failure for comparison to (**a**)

Fig. 19.5 Scanning electron micrographs of the fracture surfaces of shear specimens of (**a**) Ni-10%Fe and (**b**) Ni-10%Co
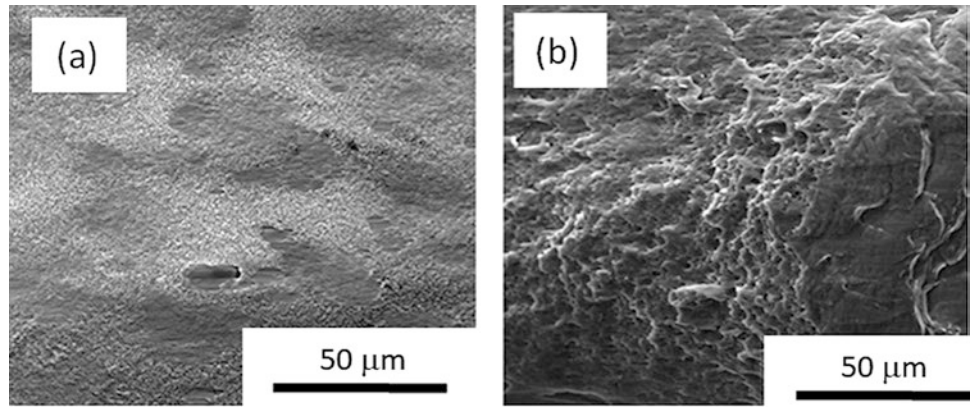

Table 19.1 Shear and tensile properties of two LIGA Ni alloys at two strain rates

Property	Quasi-static rate[a]	Quasi-static rate[a]	Intermediate rate[b]	Intermediate rate[b]
	Ni-10%Fe	Ni-10%Co	Ni-10%Fe	Ni-10%Co
Shear modulus (GPa)	48 ± 7%	33 ± 9%	40 ± 11%	37 ± 14%
Shear strength, τ_{max} (MPa)	1158 ± 2%	408 ± 1%	1205 ± 2%	455 ± 2%
Yield strength in shear (MPa)	615 ± 7%	173 ± 9%	720 ± 11%	197 ± 14%
Shear strain at fracture	0.42 ± 5%	N/A	0.54 ± 9%	N/A
Shear strain at τ_{max}	0.31 ± 7%	2.0 ± 4%	0.14 ± 7%	2.0 ± 2%
Young's modulus (GPa)	147 ± 12%	143 ± 26%	123 ± 81%	99 ± 75%
Tensile strength (MPa)	1949 ± 2%	604 ± 3%	2034 ± 2%	657 ± 3%
Yield strength (MPa)	1394 ± 12%	411 ± 26%	1609 ± 34%	432 ± 75%
True strain at fracture[*]	0.83 ± 0.11%	1.82 ± 0.31%	1.15 ± 0.03%	2.15 ± 0.22%

Values are averaged over 6 shear specimens per material/rate combination, and 3 tensile specimens per material/rate combination. The uncertainties are the measurement errors calculated from error analyses. The tensile specimens had gauge dimensions of 200 μm × 200 μm × 2 mm length
[*]The uncertainty in the true strain to fracture is the standard deviation. [a]0.001 /s. [b]1/s for tensile and 30/s for shear

exhibit rate effects but are inconclusive due to the large associated measurement uncertainties. It has been established in the conventional macroscale mechanical testing community that the Young's modulus is the least reliable property obtained from a tensile test [12] and is best measured using resonance or acoustic methods. The experimental factors that lead to large uncertainty in the Young's modulus are exacerbated for meso- and microscale tensile tests. Similar factors apply to the measurement of the shear modulus. A more detailed discussion of the measurement uncertainties associated with the tensile properties in Table 19.1, will be presented in a future paper.

Figure 19.6 shows the equivalent plastic strain at fracture for the tensile and shear specimens of the nanocrystalline Ni-10%Fe alloy, as a function of their respective stress triaxialities. The triaxiality χ is given by:

$$\chi = \frac{\sigma_H}{\sigma_{VM}} \tag{19.4}$$

where σ_H is the hydrostatic stress and σ_{VM} is the Von Mises stress. The effective strain at fracture for the shear specimens was estimated using the measured shear strain at fracture and the Von Mises yield criterion. The equivalent plastic strain for the Ni-10%Fe tensile specimens was obtained by use of finite element analysis [13]. The hydrostatic and Von Mises stresses were calculated from the principal stresses, assuming uniform and ideal stress states (i.e., pure tension for the tensile specimens and pure shear for the shear specimens). More accurate values would be obtained using finite element analysis. The tensile and shear specimens thus provide two points for constructing the fracture locus of the Ni-10%Fe alloy, as shown in Fig. 19.6, supporting the development of failure prediction models for LIGA MEMS devices. Note that Fig. 19.6 violates conventional failure prediction models for ductile metals in which the fracture strain typically increases with decreasing triaxiality. The trend in Fig. 19.6 might be due to the influence of the Lode angle parameter, as shown in recent studies at the macroscale [14].
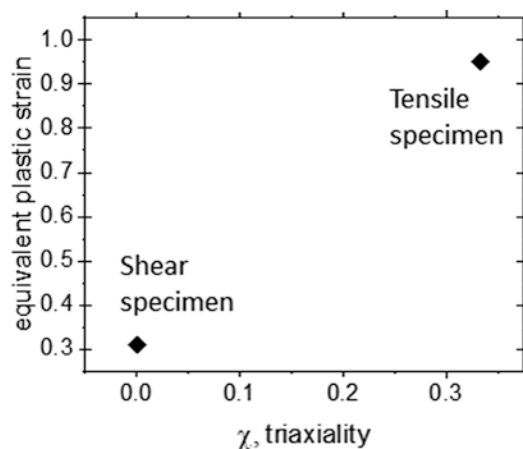
Fig. 19.6 Two points on the fracture locus for 200 μm-thick nanocrystalline Ni-10%Fe

19.4 Conclusion

We reported the design, fabrication and tensile- and shear testing of LIGA nanocrystalline Ni-10%Fe and micrograined Ni-10%Co, at two strain rates. The shear specimens were 200 μm thick and had gauge widths of 600 μm. The tensile specimens had gauge dimensions of 2 mm × 200 μm × 200 μm. Engineering shear stress vs simple shear strain curves were obtained for both alloys, at strain rates of 0.001/s and 30/s. The higher strain rate resulted in increased shear strength, tensile strength, and true strain to fracture, for both materials. We tabulated the shear properties and tensile properties along with their measurement uncertainties, and constructed part of the fracture locus for the nanocrystalline Ni-10%Fe. It is anticipated that this data may support the development of constitutive models for structural failure predictions of LIGA MEMS devices.

References

1. Becker, E.W., Ehrfeld, W., Hagmann, P., Maner, A., Munchmeyer, D.: Fabrication of microstructures with high aspect ratios and great structural heights by synchrotron radiation lithography, galvanoformung, and plastic moulding (LIGA process). Microelec. Eng. **4**, 35–36 (1986)
2. Ehrfeld, W., Bley, P., Gotz, F., Hagmann, P., Maner, A., Mohr, J., Moser, H.O., Munchmeyer, D., Schelb, W., Schmidt, D., Becker, E.W.: Fabrication of microstructures using the LIGA process. Proc. 1987 IEEE Micro Robots and Teleoperators Workshop, Hyannis, MA, pp. 11/1–11/11 (1987)
3. Schiltges, G., Gsell, D., Dual, J.: Torsional tests on microstructures: two methods to determine shear-moduli. Microsys. Tech. **5**, 22–29 (1998)
4. Schiltges, G., Dual, J.: Failure behavior of microstructures under torsional loads. J. Mech. Phys. Solids. **49**, 1021–1038 (2001)
5. Saif, M.T.A., MacDonald, N.C.: Measurement of forces and spring constants of microinstruments. Rev. Sci. Inst. **69**, 1410–1422 (1998)
6. Pantano, M.F., Espinosa, H.D., Pagnotta, L.: Mechanical characterization of materials at small length scales. J. Mech. Sci. Tech. **26**, 545–561 (2012)
7. Liew, L.A., Read, D.T., White, R.M., Barbosa, N.: U.S. Army ARDEC Joint Fuze Technology Program (JFTP) Task 2 report: quasi-static tensile tests of microfabricated electrodeposited (LIGA) Ni alloys. NIST interagency report 8182, (2018).https://doi.org/10.6028/NIST.IR.8182
8. L.A. Liew, D.T. Read, M.L. Martin, F.W. DelRio, P.E. Bradley, N. Barbosa, T.R. Christenson, J.T. Geaney. Elastic-plastic properties of mesoscale electrodeposited LIGA nickel alloys films: microscopy and mechanics. in preparation, J. Mech. Microeng. **31**, 015002, (2020)
9. ASTM Committee B07: Standard test method for shear testing of thin aluminum alloy products (ASTM B831–14). ASTM International, West Conshohocken, PA (2014)
10. Kang, J., Wilkinson, D.S., Wu, P.D., Bruhis, M., Jain, M., Embury, J.D., Mishra, R.K.: Constitutive behavior of AA5754 sheet materials at large strains. ASME J. Eng. Mat. Tech. **130**, 031004-1-5 (2008)
11. Martin, M.L., Liew, L.A., Read, D.T., Christenson, T., DelRio, F., Geaney, J.: Dominant factors for fracture at the microscale in electrodeposited nickel alloys. Sens. Actuators A: Phys. 2020;314:112239
12. Lord, J.D., Morrell, R.: Measurement Good Practice Guide No. 98: Elastic Modulus Measurement (National Physical Laboratory, UK). (2006)

13. Read, D.T., Liew, L.A., White, R.M., Barbosa, N., Geaney, J.: Measuring flow curve and failure conditions for a MEMS-scale electrodeposited nickel alloy. Mater. Res. Exp. **6**, 0950a6 (2019)
14. Bao, Y., Wierzbicki, T.: On fracture locus in the equivalent strain and stress triaxiality space. Int. J. Mech. Sci. **46**, 81–98 (2004)